ACS chemical biology

pubs.acs.org/acschemicalbiology

Article

Synthesis and Application of a Suite of 2,5-Aryl Tetrazole Photoaffinity-Based Probes for Profiling Microbial Carbohydrate and Mucin Metabolism in Gut Microbiota

Jack Russo, LaRae A. Hudson, Tulasi Rao Relangi, Abigail R. Pitts, and Aaron T. Wright*

Cite This: ACS Chem. Biol. 2026, 21, 1496–1506

Read Online

ACCESS | Metrics & More | Article Recommendations | Supporting Information

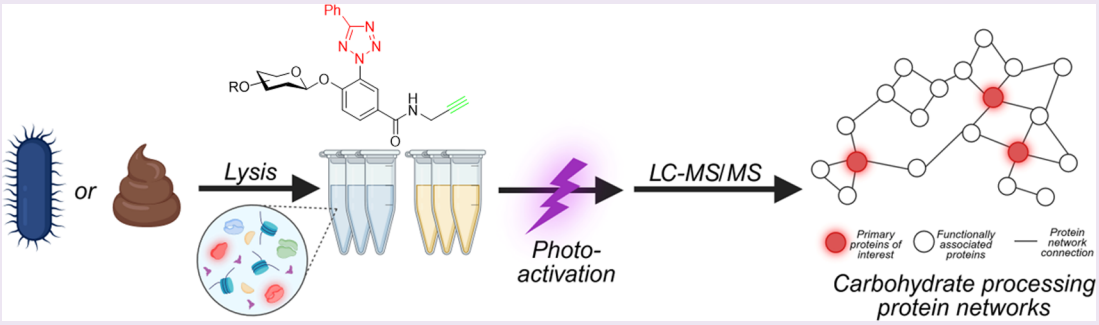

ABSTRACT: Photoaffinity-based chemoproteomics provides a strategy for interrogating protein engagement and networks within complex biological systems. In the context of carbohydrate metabolism, however, linking the probe structure to glycan-processing networks remains challenging due to the diversity and redundancy of carbohydrate-active enzymes (CAZymes). Here, we employ 2,5-tetrazoles as photoreactive groups to develop a suite of monosaccharide-bearing probes designed to capture carbohydrate-associated protein environments in gut microorganisms. Across defined bacterial cultures and human fecal lysates, tetrazole probes enriched glycoside hydrolases (GHs) and additional carbohydrate-associated proteins, including transporters and regulatory elements. Notably, enrichment profiles were functionally biased toward glycan-processing modules, despite minimal shifts in global protein abundance under different growth conditions. These findings demonstrate that tetrazole chemoproteomics complements abundance-based proteomics by reporting on glycan-associated protein engagement and organization. Together, this probe suite provides a substrate-centric approach to studying carbohydrate-processing networks in defined microbes and complex microbiomes.

INTRODUCTION

The gut microbiome plays a central role in numerous factors related to human health.[1,2] Gut microbes are important to host dietary metabolism, including polysaccharides, proteins, and vitamins.[3,4] Dysbiotic nutrient metabolism by gut microbes may promote bowel diseases and inflammatory pathologies.[5−8] Gut microbes degrade complex polysaccharides taken in by the host using a diverse array of glycoside hydrolases (GHs).[9] Humans do not have the enzymatic machinery to digest many carbohydrates found in dietary plants and are solely dependent on intestinal microbes for degradation.[10] Gut microbiome breakdown of dietary fibers is a vital phenomenon, influencing host health and disease susceptibility.[11] Additionally, dietary fiber breakdown strongly influences gut microbiome composition and resistance to pathogens.[12]

In addition to dietary fibers, gut microbes can metabolize glycans from other sources like glycolipids, human milk oligosaccharides, and glycoproteins.[13] One notable glycoprotein produced by the host, mucin, forms a protective mucosal layer between bacteria gut communities and host epithelial gut tissue.[14−16] Up to 80% of the mass of mucin is from galactose, fucose, glucosamine, galactosamine, and sialic acid.[17,18] Since mucin contains glycans, certain commensal gut bacteria express GHs that can use the mucin glycans as a nutrient source. In a healthy gut, mucin foraging promotes intestinal health and regulates mucin production. Unrestrained mucin breakdown leads to bacterial penetration to host epithelial tissues, resulting in inflammation phenotypically characterized by diseases like ulcerative colitis (UC) or Crohn's disease.[19,20]

Since bacterial GHs play such a complex role in gut health, characterization of functionally active GHs remains an important goal to understanding the etiology of gut diseases.[21] Prior literature has used affinity-based probes (*Af*BPs) to covalently modify GHs, using carbohydrates to impart

Received: March 18, 2026
Revised: May 19, 2026
Accepted: May 26, 2026
Published: June 2, 2026

https://doi.org/10.1021/acschembio.6c00268
ACS Chem. Biol. 2026, 21, 1496−1506

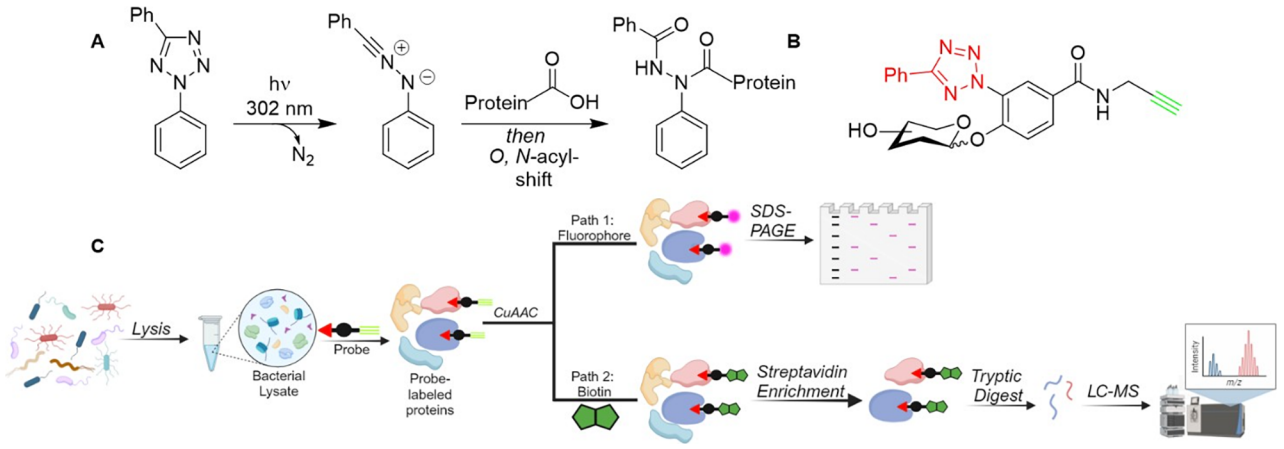

Figure 1. (A) Mechanism of photoactivation for 2,5-disubstituted tetrazoles. (B) General design for photoaffinity-based tetrazole probes in this study. All probes contain a carbohydrate recognition motif, a tetrazole reactive group (red) for covalent modification, and an alkyne handle for "click" chemistry to rhodamine/biotin-azide. (C) Chemoproteomic workflow using A*f*BPs for labeling bacterial lysate. In path 1, rhodamine is used for fluorescence imaging of labeled proteins. Path 2 shows the chemoproteomic approach, appending biotin for protein pulldown and LC-MS/MS analysis.

Scheme 1. (A) Synthetic Route for Tetrazole Probes Containing Galactose, Glucose, and Fucose Affinity Elements; (B) Alternative Tetrazole Probe Synthesis for *N*-Acetyl Glucosamine; (C) Suite of Tetrazole and Carbohydrate Containing Probes Used in This Study

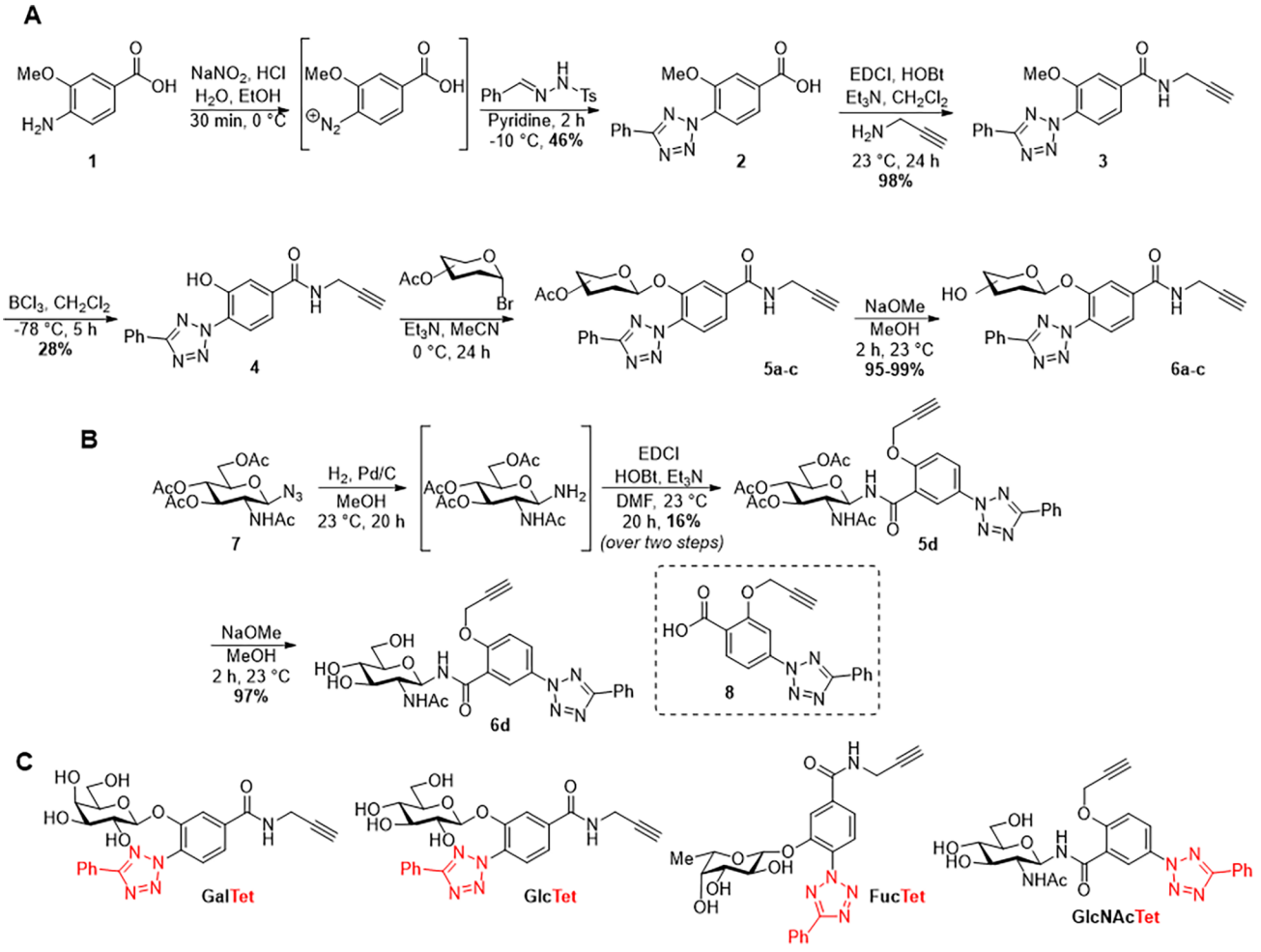

specificity; however, off-target protein enrichment remains a persistent issue when seeking to investigate specific microbial GH activity.[22,23] Monosaccharide probes functionalized with electrophilic α-halo acetamides often enrich proteins by high abundance.[24−26] Additionally, activity-based reactive groups like cyclophellitol probes only target retaining GHs and cannot

https://doi.org/10.1021/acschembio.6c00268
ACS Chem. Biol. 2026, 21, 1496−1506

capture carbohydrate-related metabolism or transport pathways.[27−29]

Rather than rely on poorly annotated genomes, *Af*BPs with photo-crosslinkers, or light-activated reactive groups, can be implemented to broadly investigate proteins in metabolism or transport. The choice of photo cross-linker is vital to probe specificity, but all have intrinsic limitations.[30] Diazirines, frequently extolled for their small size and high reactivity, operate by competing mechanisms of labeling. In addition to carbene formation, prior work has shown that diazirines can isomerize to the linear diazo, potentially negatively biasing labeling to acidic residues on protein surfaces. Generated carbenes also undergo 1,2-H-migration to the alkene, leading to nonproductive probe degradation.[30−33]

To increase probe labeling of GHs and minimize undesirable protein enrichment, an overlooked photoreactive moiety, 2,5-tetrazole, was incorporated.[34] Mechanistically, UV activation results in expulsion of N_2 and the formation of a reactive nitrilimine intermediate (Figure 1A).[35] The highly reactive nitrilimine species preferentially labels carboxylates (Asp and Glu amino acids).[36−38] After reaction with acidic amino acid residues, the product is stable in aqueous conditions, allowing for gel-based analysis or chemoproteomics. Prior research has demonstrated the amino acid selectivity of tetrazoles by global labeling of acidic amino acids in living bacteria, also highlighting the bio-orthogonality of this reactive group.[39,40]

Inspired by this work, we sought to develop *Af*BPs with tetrazole photoreactive groups and carbohydrate affinity scaffolds to profile GHs and carbohydrate-related proteins in commensal gut microbes (Figure 1B). We hypothesized that by adding a monosaccharide to a tetrazole-based probe, we could selectively enrich GHs, alongside transporters and transferases. The tetrazole probes described here are designed to enable functional profiling of carbohydrate-processing systems rather than to act as substrate-specific glycosidase reporters or irreversible active-site inhibitors.

In microbial metabolism, GHs function within coordinated assemblies that include multiple GH families, carbohydrate-binding modules, transporters, and regulatory proteins.[41,42] Accordingly, probe engagement reflects interactions within carbohydrate metabolism pathways, rather than exclusive recognition of a single monosaccharide substrate. Photoactivation enables the covalent capture of enzymes and associated proteins that are functionally proximal to the carbohydrate affinity element. Thereby, tetrazole probes provide a systems-level view of which carbohydrate-degrading functions are engaged.

Described herein are the synthesis and characterization of a suite of tetrazole probes for investigating microbial enzymes associated with mucin foraging and carbohydrate metabolism. Facile swapping of the affinity element with different carbohydrates also enables collection of unique GH enrichment targets respective of each probe. All probes are CuAAC, or "click" chemistry compatible (Figure 1C), and were validated by SDS-PAGE and liquid chromatograph tandem mass spectrometry (LC-MS/MS)-based chemoproteomics.

RESULTS AND DISCUSSION

Synthesis of Tetrazole Probes with Diverse Affinity Elements

When designing tetrazole probes, we sought to develop a probe suite incorporating the carbohydrates present in fiber or mucin to target different GHs and carbohydrate-associated proteins and transporters (Scheme 1A). All probes started from commercially available acid **1** and generated the diazonium salt, followed by reaction with benzaldehyde phenylsulfonylhydrazone. With the tetrazole reactive group in place, we coupled acid **2** with propargyl amine, yielding amide **3**. Demethylation with BCl_3, followed by glycosylation with the desired anomeric halide yielded probes **5a−c**. This synthetic route enabled synthesis of probes containing galactose, glucose, and fucose affinity elements, all with selectivity for the β-anomer. Final deprotection using Zemplen's conditions yielded final probes **6a−c**. We note here that probes synthesized so far are O-aryl glycosides, which are potentially rapidly cleaved by GHs. In fact, electron-withdrawing nitrophenol (NP) glycosides have been used to study the kinetics of many GHs; however, we presume that the large steric bulk of the aglycone here precludes the rapid hydrolysis rate observed with NP substrates. Future work will continue to optimize the linkage between the sugar moiety and aglycone.

The synthetic approach was then applied to the anomeric halide of *N*-acetyl glucosamine; however, only recovered starting material was detected. Alternative glycosylation methods using phase-transfer conditions or Lewis acids also failed. To circumvent this issue, we instead synthesized the anomeric amine (Scheme 1B), serving as a synthetic handle for an amide coupling with tetrazole partner **8**. Additionally, the potential hydrolysis issues cited above are removed with this probe, now containing a less readily cleavable amide linkage. With an *N*-acetyl glucosamine probe in hand, deacetylation yielded the final probe **6d** for gel and proteomic validation. With all probes synthesized (Scheme 1C), we proceeded to test the reactivity of all compounds in bacterial lysate.

Probe Reactivity and Gel Analysis

Probe reactivity was tested in lysate preparations of two commensal gut bacteria known for robust mucin and carbohydrate metabolism: *Bacteroides thetaiotaomicron* (*Bt*) and *Akkermansia muciniphila* (*Am*). For fluorescence readout of labeled proteins (path 1, Figure 1), labeling of **6a** was compared over a range of concentrations and (Figure S8) irradiation times, observing increased labeling intensity with time (Figure S9). No obvious differences in labeling patterns were found across probe, except varied intensity. Additionally, ranges in incubation time also resulted in minimal differences to labeling intensities (Figure S10). To mechanistically confirm that labeling is driven by an *in situ* generated nitrilimine, probe **6a** was subjected to photoirradiation in PBS. Addition of the "pre"-activated probe to lysate displayed only background labeling, confirming that probe labeling is from an *in situ* photogenerated electrophile (Figure S13). We briefly sought to test if the tetrazole probes were inhibiting GH activity. Tests of galactosidase activity in *Escherichia coli* lysate show probe labeling results in non-significant reduction in overall galactosidase activity, relative to nonlabeled (Figure S6).

As all probes showed promising results by gel-based analysis (for probe comparisons in each lysate, see Figures S11 and 12), we then proceeded to test their reactivity using the LC-MS/MS chemoproteomics workflow shown in path 2 of Figure 1. Additionally, global proteomic data for each bacterial lysate for comparison to probe data were collected.

Proteomics of *B. thetaiotaomicron* and *A. muciniphila*

Global proteomic measurements were performed on the lysate of both bacteria (Figure 2A,B; please see Table S1 and

https://doi.org/10.1021/acschembio.6c00268
ACS Chem. Biol. 2026, 21, 1496−1506

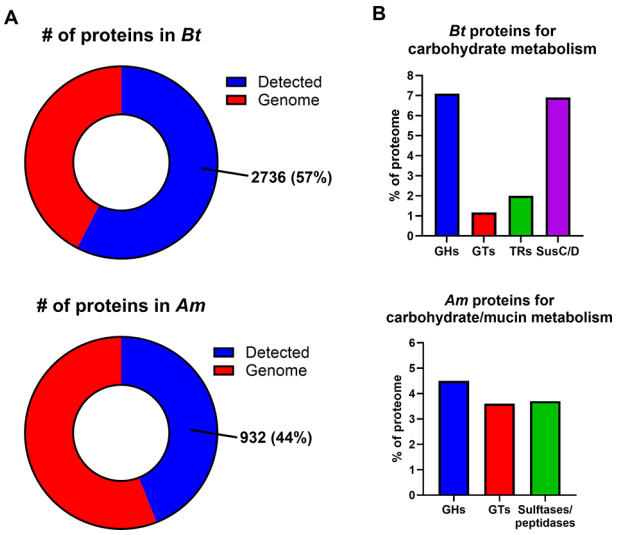

Figure 2. Global proteomic data from *Bt* and *Am* lysate ($n = 4$), using data-dependent acquisition (DDA). (A) The total number of proteins detected in *Bt* was 2736, 57% of the potential number of proteins from the genome. For *Am*, 932 proteins were detected, or 44% of the genome. (B) Percent of proteins in the proteome for carbohydrate metabolism. TRs are transcriptional regulators for carbohydrate metabolism.

Documents S1 and S2 for more information). For *Bt*, across four replicates, more than 2000 proteins were detected. To assess proteome investment in carbohydrate-associated functions, protein abundances were quantified using intensity-based normalization with category-specific intensities summed and normalized to the total detected proteome intensity averaged across replicates. This analysis revealed that a substantial fraction of the expressed proteome is devoted to carbohydrate acquisition and metabolism, including polysaccharide transporters (SusC/D) (7.0%), GHs (7.1%), and glycosyltransferases (1.2%). For *Am*, 932 proteins were measured. Similar to *Bt*, *Am* devotes a large portion of its proteome to carbohydrate and mucin degradation, including GHs (4.3%), GTs (3.2%), and sulfatases/peptidases (3.4%). Collectively, these data provide a framework for interpreting chemoproteomics data in *Bt* and *Am* lysate (for additional information on global data, see Table S1 and Figure S2).

LC-MS/MS Chemoproteomics Using the Tetrazole Probe Suite

Each probe was added to the lysates from each microbe. Following protein labeling, probes underwent CuAAC with biotin-azide, enrichment with streptavidin agarose resin, and trypsin digestion. Following the LC-MS/MS run, unique peptides were matched to proteins and compared against probe controls that did not receive UV activation.

During this study, it became pertinent to discern if enrichment was guided by the affinity element or the tetrazole photo-crosslinker scaffold. Compound **3**, which bears no carbohydrate affinity region but all other necessary components for chemoproteomics, was also subjected to analysis. This enabled collection of a tetrazole "photome", a list of noncarbohydrate-specific protein binding, which can then be compared to previous probe results to identify proteins truly enriched from the affinity element.[43]

In *Am* lysate, compound **3** significantly enriched proteins that were highly abundant proteins such as ribosomal subunits and DNA replication proteins. To distinguish between background photome labeling and affinity labeling, all significant protein hits from tetrazole probes were then compared to photome proteins. After statistical filtering of proteins also found in the photome (Figure S3), a list of affinity hits was generated for each *Af*BP. Importantly, GHs identified in probe-enriched data sets were absent from the sugar-free photome control, indicating that their enrichment depends on the carbohydrate affinity element. We note that non-GH proteins are also enriched. These proteins may reflect labeling of non-CAZyme proteins with putative roles in carbohydrate metabolism or true nonspecific labeling events. Further work is still needed to distinguish between protein affinity networks and nonselective labeling.

GalTet enriched two galactosidases (Figure 3A), GH27 and 35, identified as α- and β-galactosidase, respectively. GH27 has previously been shown to be a galactosidase with preference for "animal type" substrates over plant, indicating that this GH enriched is more likely associated with mucin metabolism than dietary fiber breakdown.[44] GlcTet enriched multiple *N*-acetyl

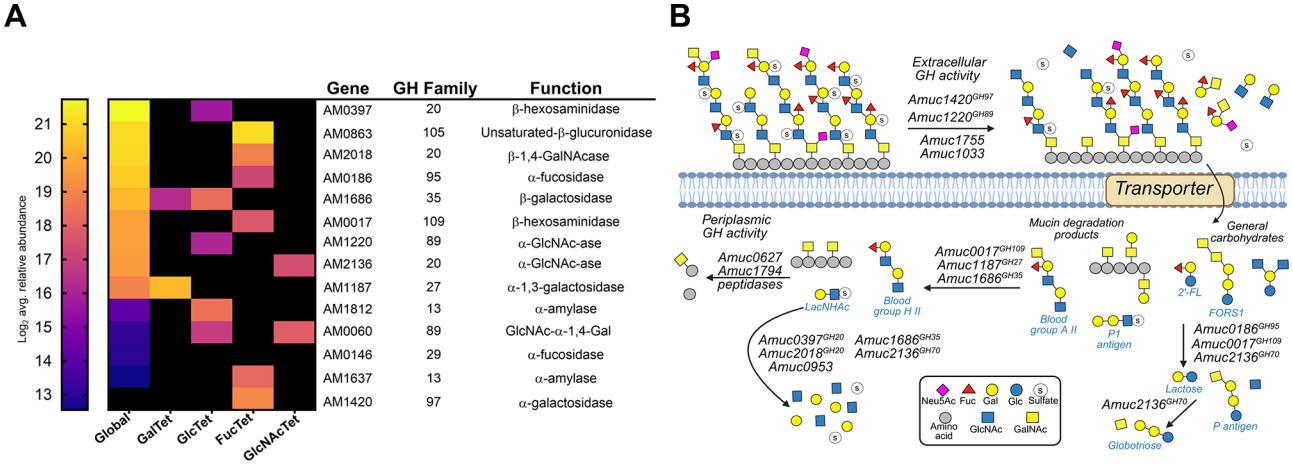

Figure 3. (A) Global proteomics data compared to chemoproteomics data from tetrazole probes in *A. muciniphila* lysate. All data represents the $\log_2$ average relative abundance of detected proteins. Black cells represent undetected proteins. Functions are assigned according to the CAZY database. (B) Proposed functional degradation pathway of mucin from tetrazole probes.[44]

https://doi.org/10.1021/acschembio.6c00268
ACS Chem. Biol. 2026, 21, 1496−1506

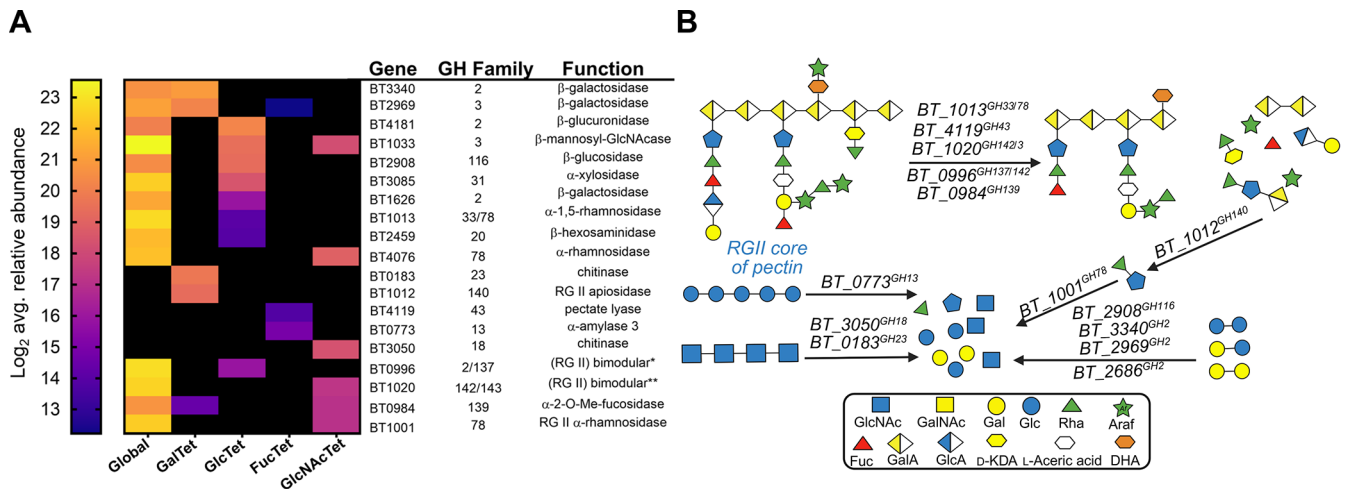

Figure 4. (A) Global proteomics data compared to chemoproteomics data from tetrazole probes **6a**−**d** in *B. thetaiotaomicron*. Black cells represent undetected proteins. Functions are assigned according to the CAZY database (PH = phosphorylase). (B) Schematic depiction of representative GHs enriched by probes **6a**−**d** in *B. thetaiotaomicron*. *GH with known bimodular function as a β-L-arabinofuranosidase/β-glucuronidase (cleaves L-Araf-β-1,2-L-Rha). **Bimodular (Dha) hydrolase/β-L-arabinofuranosidase.[41]

hexosaminidases, indicating that the 2′-position is not significantly contributing to the affinity element. By utilizing *Af*BPs, we also capture protein−protein interactions relevant to mucin breakdown. Importantly, probes Gal/GlcTet enrich sulfatases and peptidases involved in mucin breakdown. Next, FucTet enriched a diverse number of GHs, like GH13, 20, and 109. These are highly abundant and do not have fucose metabolizing capabilities; however, GH95, an α-fucosidase, was significantly enriched, along with other fucose-related enzymes like fucose isomerase and 6-phosphofructokinase. Lastly, GlcNAcTet significantly enriched two GHs, both associated with hexosaminidase metabolism. Both GHs enriched match the affinity element of GlcNAcTet, highlighting how probe enrichment profiles can be tuned with small alterations in carbohydrate structure.

To facilitate interpretation of the heatmap data, we overlaid probe-enriched enzymes onto a schematic representation of mucin *O*-glycan degradation derived from prior genetic and biochemical studies of *Am* (Figure 3B).[44] This organism was selected as a model because its mucin degradation machinery has been extensively characterized at the genomic and transcriptomic levels. This made it an ideal system to evaluate whether tetrazole probes capture enzymes that have been previously implicated in mucin breakdown. The enrichment of GH33, GH20, GH84, and GH18 and related enzymes is consistent with known mucin *O*-glycan trimming steps. However, probe enrichment alone does not establish catalytic involvement in mucin degradation, and we therefore interpret these results as evidence of carbohydrate-associated proximity engagement rather than functional validation.

Next, the tetrazole probe suite was applied to *Bt* lysate, in addition to compound **3** for photome profiling (Figure S4). Like *Am* data, the photome consisted mainly of housekeeping proteins (ribosomal subunits, DNA replications proteins, etc.), with no GHs significantly enriched. Galactose probe, GalTet, enriched two β-galactosidases in the GH2 family (Figure 4A). Additionally, it enriched for GH140, an aposidase for rhamnogalacturonan II (RG II), which was also undetected by global protein profiling. GH140 is a vital enzyme for pectin breakdown, meaning the probe enriches GHs for fiber degradation. Similarly, GH139 was enriched, shown previously to cleave methylated fucose from the RGII core of pectin. While not strictly a galactosidase, previous work has demonstrated this enzyme to contain galactose recognition motifs, since the neighboring sugar in the pectin chain is galactose.[41] Glucose probe, GlcTet, enriched several GHs with diverse functions. Two GHs enriched by GlcTet also have important functions for dietary fiber breakdown (GH31 and GH33/78). Compared to other probes, GlcTet had a noticeably increased number of total proteins enriched, the majority of which are not strictly glucosidases. We observed that many of these proteins are clustered around bacterial glucose metabolism, like glycolysis and pentose phosphate pathways (see the SI, Figure S5). Therefore, though many of these enriched proteins appear to be "off-target", the centrality of glucose in bacterial metabolism potentially biases overall enriched proteins to plausible biological pathways.

Fucose probe, FucTet, enriched for three GHs, two not detected by global data. Despite only having a monosaccharide affinity element, FucTet enriched for GHs associated with larger dietary fiber breakdown, such as pectate (GH43) and amylase (GH13). Last, GlcNAcTet-enriched GH18, a chitinase not detected in global samples. Interestingly, chitinase, meant to break down repeating units of *N*-acetyl glucosamine, is being selectively enriched by a probe containing the same sugar motif.

The overall GH enrichment profile between each tetrazole probe has two critical trends: (1) some GHs are undetectable in the global proteomic data, and (2) each respective affinity element results in a unique GH enrichment profile. Additionally, many of the GHs enriched are for dietary fiber breakdown like pectin, starch, or chitin. As depicted in Figure 4B, these data support the use of tetrazole probes to enrich carbohydrate-associated networks as tools to enrich carbohydrate protein networks for microbial dietary fiber breakdown. Furthermore, we assert that the combination of global proteomics and enriched GHs provides a more comprehensive profile of proteins in carbohydrate metabolism in *Bt*.

Importantly, many of the probes had unanticipated protein targets given the respective carbohydrate affinity element, warranting further investigation of the degree of selectivity of the tetrazole probes. In *Am* lysate, each probe enriched for

https://doi.org/10.1021/acschembio.6c00268
ACS Chem. Biol. 2026, 21, 1496−1506

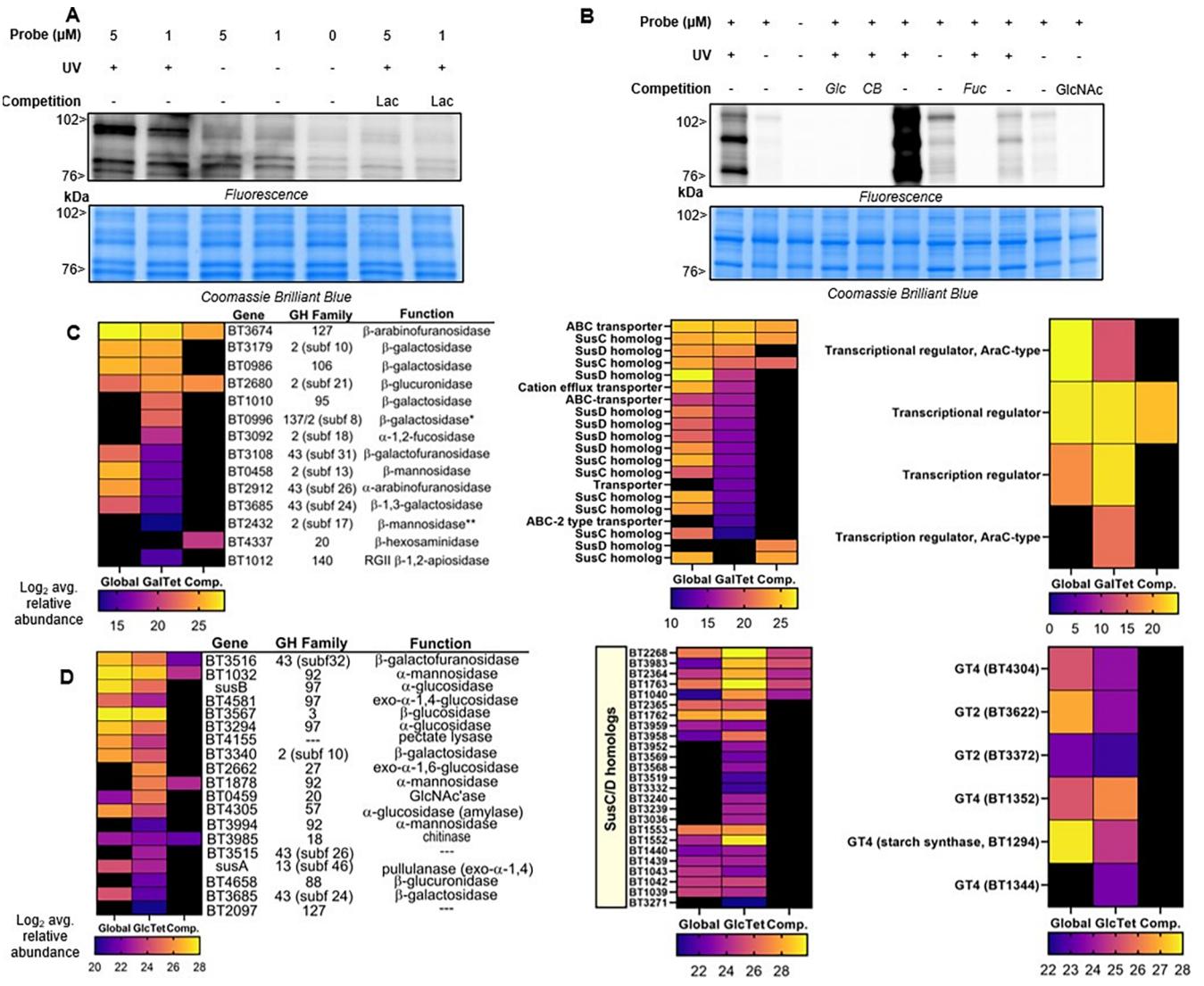

Figure 5. (A) Fluorescence image of GalTet in *Bt* lysate (*Bt* grown in the presence of galactose and lactose), with protein stain below. Lactose (Lac) was used as a competitor, which was preincubated at 100× probe concentration prior to probe addition and photoactivation. (B) Fluorescence image of GlcTet, FucTet, and GlcNAcTet. For GlcTet, lysate from *Bt* grown with starch and cellobiose (CB) was used.For FucTet and GlcNAcTet, *Bt* grown with mucin was used. Respective competitors were preincubated at 100× probe concentration prior to probe addition (1 μM) and photoactivation. (C) LC-MS/MS chemoproteomic data of GalTet alongside competition (comp.) with lactose. Enriched GHs (left), transporters (middle), and carbohydrate-related transcriptional regulators (right) shown. (D) LC-MS/MS chemoproteomic data of GlcTet alongside competition with cellobiose. Enriched GHs (left), transporters (middle), and GTs (right) shown.

only a handful of GHs, alongside other carbohydrate-related proteins. There was still overall enrichment of proteins primarily associated with housekeeping functions, such as ribosomal subunits, DNA replication proteins, and ATPases. The same trend was observed to a greater extent in *Bt* lysate, particularly with probes containing a glucose-like affinity scaffold (GlcTet and GlcNAcTet). For example, GlcTet overall enriched <150 proteins, with only 24 associated with carbohydrate metabolism, and eight GHs. We attribute many of these off-target hits to highly abundant housekeeping proteins, which is a common and frequently unavoidable enrichment trend in photoaffinity labeling.

To address specificity concerns, we conducted several control experiments. First, bacterial lysate was heat-shocked to discern if labeling is driven by functionally active proteins. Next, we used competition experiments, either with known reversible inhibitors like phenylethyl β-thiogalactoside (PETG) or the native mono- or disaccharide sugars (for example, galactose or lactose). We also took advantage of polysaccharide utilization loci (PUL) induction in *Bt* by culturing in the presence of lactose, starch, or mucin. Fluorescence readouts from probe-labeled proteins by GalTet produce significantly more intense banding when exposed to UV light versus not (Figure 5A). It is also likely to label active enzymes in the lysate, as heat shock (*hs*) controls greatly reduced labeling. Preincubation with PETG also diminished fluorescent intensities (see the SI, Figures S14 and S15). Lastly, competitive labeling with galactose or lactose, the natural ligands of β-galactosidases, also significantly decreased labeling. Together, these results suggest that probe GalTet is labeling functionally active proteins, and the probe is competitive for β-galactosidases in this lysate. The same competition experiments were conducted with GlcTet (Figure 5B). Competition

https://doi.org/10.1021/acschembio.6c00268
ACS Chem. Biol. 2026, 21, 1496−1506

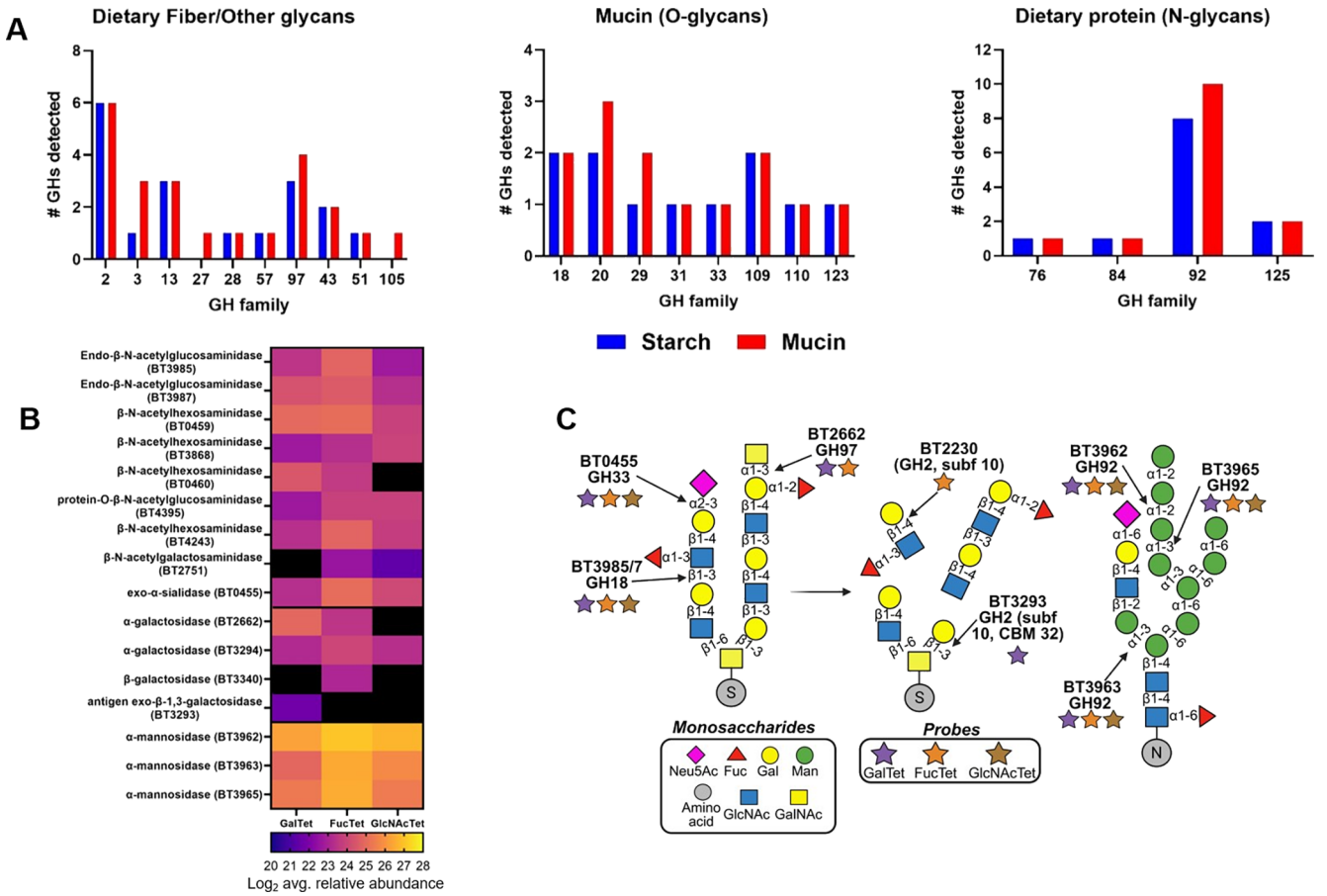

Figure 6. (A) Detected GHs per GH family in *B. thetaiotmicron* cultures grown on starch versus mucin via global proteomics ($n = 4$). GH families were broadly categorized based on annotations from the CAZy and dbCAN databases. (B) Enriched GHs from tetrazole probe in *B. thetaiotmicron* lysate that was cultured with mucin. (C) Schematic representation of mucin *O*-glycan (left) and mannose-rich *N*-glycan (right) processing pathways. Selected enzymes enriched by Gal/Fuc/GlcNAcTet are indicated by colored stars.

with cellobiose (CB) showed reduction in labeling intensities compared to noncompetitive labeling.

The same competition experiments were performed with FucTet and GlcNAcTet probes in lysates from *Bt* cultured in media containing mucin. Like previous PUL implementation, growth on mucin promoted increased carbohydrate metabolism around fucose and GlcNAc. We used the monosaccharides fucose and *N*-acetyl glucosamine for competition labeling, representative of enzyme product inhibition.[45] As shown by Figure 5B, protein labeling by both FucTet and GlcNAcTet is competitively inhibited by the respective monosaccharides as evidenced by the significant reduction in labeling (see the SI, Figure S16).

After demonstrating competitive labeling of tetrazole probes, we validated GalTet and GlcTet competitive labeling with LC-MS/MS chemoproteomics (Figure 5C,D). Several enriched GHs by GalTet are annotated as β-galactosidases, and comparison to global proteomics highlights labeling by GalTet is not driven by high abundance, with five GHs undetectable by global profiling. Competition with lactose substantially reduced labeling for all enriched galactosidases, indicative that GalTet is competitive for the natural ligand (lactose) for the active site of galactosidases. Like previous data, a few enriched GHs are not annotated as galactosidases. For instance, BT2432 is functionally annotated as a mannosidase; however, this GH also contains carbohydrate-binding motif (CBM) 32, recognizing galactose and lactose according to the CAZy database.[46,47] While functionally this GH is not a galactosidase, we attribute the "off-target" labeling to the CBM.

In addition to galactosidases, GalTet also captured enzymes annotated as β-glucuronidases, α-fucosidases, and RGII apiosidases. The labeling of GHs beyond those with strict galactose specificity likely reflects the photoaffinity-based mechanism. GalTet can cross-link not only to directly engaged catalytic residues but also to proteins in close spatial proximity. In the context of PULs, CAZymes frequently function within multienzyme assemblies and Sus-associated complexes, where galactosidases, glucuronidases, fucosidases, and RGII-processing enzymes act coordinately on structurally related glycans. From this perspective, enrichment of these additional GHs is a function of protein−protein interaction networks rather than nonspecific labeling. In fact, GalTet competitively enriched a plethora of carbohydrate transporters and SusC/D homologues, alongside AraC-type transcriptional regulators involved in PUL transcription. These observations highlight that probe labeling extends beyond individual catalytic enzymes to encompass associated transport and regulatory proteins. Importantly, the GalTet probe can capture directly engaging GHs and associated proteins, a key advantage of tetrazole based-photoaffinity probes.

In addition to GalTet, we performed competitive chemoproteomics using GlcTet with cellobiose as the competitor (Figure 5D). Multiple GHs annotated as glucosidases were enriched across distinct GH families. Notably, enzymes

https://doi.org/10.1021/acschembio.6c00268
ACS Chem. Biol. 2026, 21, 1496−1506

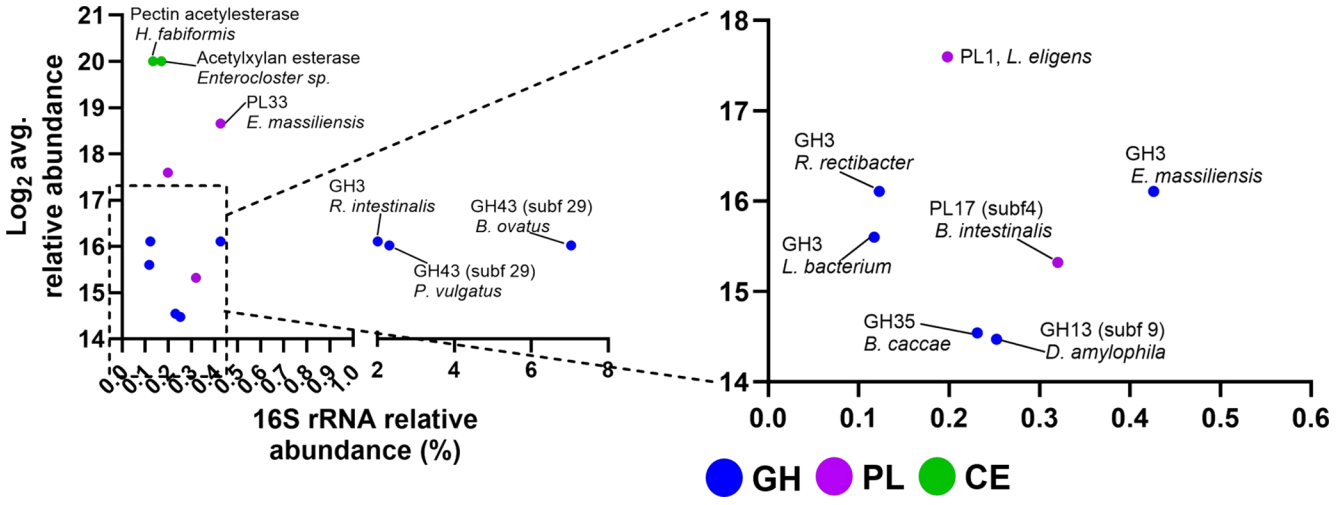

Figure 7. Enriched CAZymes by the GalTet probe (n = 4) in lysate from human stool in comparison to 16S rRNA relative abundances. For a CAZyme to be identified, values must have be present in a minimum of 75% of the replicates and completely absent in no UV controls. Glycoside hydrolases (GHs), polysaccharide lyases (PLs), and carbohydrates esterases (CEs) shown.

targeting higher-order α-glucans, including an amylase and a pullulanase, were enriched. Competitive labeling with cellobiose completely eliminated probe labeling. Although GlcTet contains a β-linked glucose scaffold, several α-glucosidases were competitively enriched. Again, these probes rely on photoinduced proximity labeling, rather than mechanism-based covalent capture. Thus, enrichment reflects proximity within carbohydrate-binding or catalytic environments rather than strict stereochemical recognition. Because of the mechanism of tetrazole activation by UV, we would not expect stereoselective labeling, and enrichment of α-acting enzymes is consistent with photoaffinity labeling.

Consistent with GalTet, GlcTet also enriched GHs not strictly annotated as glucosidases, including mannosidases, galactosidases, and *N*-acetylglucosaminidases. The tetrazole substitution at the anomeric position of the glucose affinity element likely alters hydrogen-bonding and steric interactions within the catalytic cleft, potentially broadening engagement to enzymes that accommodate related hexose configurations. While several mannosidases were enriched, global proteomics revealed these enzymes to be highly abundant under the growth conditions, likely reflecting mannose derived from host glycoconjugates. We therefore interpret enrichment of some mannosidases as influenced by protein abundance.

Beyond GHs, GlcTet enriched additional carbohydrate-associated proteins (Figure 5D, middle and right panels). Several TonB-dependent transporters and SusC/SusD homologues were competitively labeled, indicating probe engagement with outer membrane glycan-binding and transport machinery. Importantly, many of these Sus homologues are encoded within the same polysaccharide utilization loci (PULs) as enriched GHs, suggesting coordinated capture of functionally linked carbohydrate-utilization systems. A subset of glycosyltransferases (GTs) was also enriched, further supporting the idea that photoaffinity labeling extends beyond catalytic hydrolases to proteins embedded within broader glycan-processing networks.

Having established that tetrazole-based photoaffinity probes competitively enrich GHs and associated transport and regulatory proteins, we next applied this platform to a biologically relevant glycan environment. *B. thetaiotaomicron* is a model host-glycan forager with multiple PULs implicated in mucin *O*-glycan degradation. While these loci and their regulatory responses have been extensively characterized at the genomic and transcriptomic levels, transcriptional activation does not necessarily reflect protein abundance, complex assembly, or functional engagement at the proteome level. We therefore cultured *Bt* in a mucin-containing medium and combined global proteomics with tetrazole-based chemoproteomics to investigate carbohydrate-associated protein abundance and mucin-responsive protein networks.

Comparison of global proteomics from *Bt* cultures grown on starch versus mucin showed only modest differences in GH family distribution (Figure 6A). For both cultures, *Bt* maintained a large carbohydrate-processing profile, with respective carbon source exerting minimal impact on GH family representation. Similar trends were observed for sulfatases, peptidases, and SusC/D homologues, indicating that global abundance profiles are largely preserved under these rich-medium growth conditions. We note for both cultures a prominent number of mannosidases, presumably for host-glycan foraging from animal-derived proteins in rich media. The persistence of mannosidases may reflect a more constitutive capacity for glycoprotein glycan foraging. Such baseline expression is consistent with the gut microbiome environment, as microbes also encounter dietary glycoproteins in addition to dietary fibers and host glycoproteins.

These findings indicate that abundance-based global proteomics alone does not fully capture glycan engagement or the organization of carbohydrate metabolism under different carbon sources. To interrogate glycan networks directly, we applied tetrazole probes bearing mucin-relevant affinity elements to *Bt* cultures grown on mucin. Under mucin growth conditions, all three probes enriched GHs associated with mucin *O*-glycan metabolism (Figure 6B). GHs involved in terminal glycan trimming were prominently captured, including GH33 exo-α-sialidase (BT0455), GH123 β-*N*-acetylgalactosaminidase (BT2751), multiple GH20 β-*N*-acetylhexosaminidases (BT0459, BT3868, and BT4243), GH84 protein *O*-β-*N*-acetylglucosaminidase (BT4395), and GH18 endo-β-*N*-acetylglucosaminidase-like enzymes (BT3985, BT3987).

https://doi.org/10.1021/acschembio.6c00268
ACS Chem. Biol. 2026, 21, 1496−1506

These activities correspond to removal of terminal glycan residues in mucin.

Notably, the galactose-bearing probe enriched both α-galactosidases (BT2662 and BT3294) and exo-α-sialidase (BT0455). Because sialic acid removal exposes underlying galactose residues during mucin *O*-glycan processing, the co-capture of these enzymes is consistent with sequential glycan trimming steps operating within coordinated assemblies. Similarly, GlcNAcTet enriched multiple GlcNAc- and GalNAc-processing enzymes, supporting engagement of core glycan metabolism.

In addition to *O*-glycan-associated GHs, multiple GH92 α-mannosidases were coenriched across probes. Mannose-rich *N*-glycans share structural features with mucin *O*-glycans, including branching architectures and neighboring GlcNAc, galactose, and capping sialic acid residues. The enrichment of GH92 enzymes alongside *O*-glycan trimming activities may reflect coordinated engagement of structurally related glycan motifs rather than independent substrate pools. Their shared enrichment supports a model in which tetrazole probes report glycan-processing assemblies for both mucin-type *O*-glycans and mannose-rich *N*-glycans (Figure 6C).

After probe enrichment analysis in single-organism gut commensals, we advanced to testing our probes in a complex human microbiome sample from stool. GalTet and control probe **3** were applied to human fecal lysate to confirm affinity versus photomethylation in a more complex sample (Figure 7). Data were processed using an in-house database from 16S rRNA from the same stool sample. The GalTet probe enriched a total of 322 proteins, with 170 enriched in the photome (see the SI, Figure S9). Of the 65 shared proteins between the two groups, no CAZymes were detected, along with none being enriched independently by **3**. Thus, the galactose moiety of GalTet in fecal lysate significantly alters affinity with respect to the photome.

Enriched CAZymes by GalTet spanned GHs, PLs, and CEs Notably, enriched proteins were derived from organisms present at both low and moderate 16S relative abundances (0.1−7%), meaning that enrichment did not correlate with organismal abundance. Several β-galactosidases (GH3 and GH35) were enriched, alongside PLs for pectin and heparinase (PL1 and 17). Notably, enriched galactosidases co-occurred with GH43 from *B. ovatus* and *P. vulgatus*. GH family 43 is often related to breakdown of arabinoxylan, a process that releases galactose-containing side chains or generates galactose accessible environments. The concurrent enrichment of galactosidases and xylan-active GH43 enzymes suggests that galactose-processing modules in the human gut may be functionally embedded within broader arabinoxylan degradation networks. Similar trends from single-organism labeling were also observed in feces, with enrichment of several putative proteins related to carbohydrate metabolism, including proteins for glycolysis, ATP synthesis, and the pentose phosphate pathway. Future experiments will continue to investigate if these enriched proteins represent nonselective labeling or capture of protein affinity networks.

These data support a model in which GalTet captures carbohydrate-processing assemblies in the human gut, linking galactose metabolism to xylan degradation pathways across diverse gut bacteria.

CONCLUSIONS

In this study, tetrazole-based *Af*BPs were used to interrogate glycan-associated protein environments in both defined bacterial cultures and complex human fecal lysates. While global proteomics revealed minimal shifts in CAZy abundance under different growth conditions, chemoproteomics labeling captured coordinated glycan-processing modules that were not apparent from abundance-based metrics alone. In *Bacteroides* cultures, probes enriched sequential mucin trimming enzymes, supporting proximity-based organization of *O*-glycan metabolism. In fecal lysate, GalTet enriched CAZymes and associated transport and regulatory proteins across taxa, independent of organismal abundance, and distinct from the sugar-free photome control. We still note background labeling of abundant proteins, underscoring the need for future work to consider more controls; however, these probes provide complementary affinity-based readouts of glycan engagement beyond protein abundance alone.

Future work will expand this platform by incorporating tetrazole probes bearing larger di- and trisaccharide affinity elements to better mimic native glycan motifs, short linkers between the glycan and tetrazole reactive groups. Additionally, we note that Gal-, Glc-, and FucTet probes are aryl glycosides, which are potentially rapidly cleaved *in situ*, leading to off-target labeling. Nonhydrolyzable probes like GlcNAcTet could potentially address this limitation, but further work is required to determine the impacts of an activated aryl glycoside in tetrazole-based photoaffinity labeling. The implementation of the current iteration of tetrazole probes in new systems requires careful controls for validation, many of which were performed here.

ASSOCIATED CONTENT

Supporting Information

The Supporting Information is available free of charge at https://pubs.acs.org/doi/10.1021/acschembio.6c00268.

Probe synthesis and characterization; all gels with controls; NMR spectra for probes and intermediates; other supplemental protein hits for all probes; data for GH families from global proteomics; and raw data available via MassIVE (MassIVE MSV000098948) (PDF)

All global or chemoproteomics data (XLSX)

All global or chemoproteomics data after normalization and filtering (XLSX)

AUTHOR INFORMATION

Corresponding Author

Aaron T. Wright − *Department of Chemistry & Biochemistry and Department of Biology, Baylor University, Waco, Texas 76706, United States;* orcid.org/0000-0002-3172-5253; Email: a_wright@baylor.edu

Authors

Jack Russo − *Department of Chemistry & Biochemistry, Baylor University, Waco, Texas 76706, United States*

LaRae A. Hudson − *Department of Biology, Baylor University, Waco, Texas 76706, United States*

Tulasi Rao Relangi − *Department of Biology, Baylor University, Waco, Texas 76706, United States*

https://doi.org/10.1021/acschembio.6c00268
ACS Chem. Biol. 2026, 21, 1496−1506

Abigail R. Pitts − *Department of Biology, Baylor University, Waco, Texas 76706, United States;* orcid.org/0009-0006-7380-5426

Complete contact information is available at: https://pubs.acs.org/10.1021/acschembio.6c00268

Notes

The authors declare no competing financial interest.

■ ACKNOWLEDGMENTS

The authors acknowledge the use of core facilities provided at Baylor University. Compound characterization was performed with the assistance of the NMR facilities and expertise help from Dr. Xu. Proteomic data was collected within Baylor's Mass Spectrometry Center, with instrument assistance provided by Dr. Chinthaka Seneviratne and Dr. Alejandro J. Ramirez. SDS-PAGE assistance was provided courtesy of Dr. Michelle Nemec of Baylor's Molecular Biosciences Center. We acknowledge funding from the NIH NICCH grant #R01AT013241. We acknowledge the use of BioRender to prepare certain figures.

■ REFERENCES

(1) Gilbert, J. A.; Lynch, S. V. Community Ecology as a Framework for Human Microbiome Research. *Nat. Med.* **2019**, *25* (6), 884−889.
(2) Lozupone, C. A.; Stombaugh, J. I.; Gordon, J. I.; Jansson, J. K.; Knight, R. Diversity, Stability and Resilience of the Human Gut Microbiota. *Nature* **2012**, *489* (7415), 220−230.
(3) Wilmes, P.; Martin-Gallausiaux, C.; Ostaszewski, M.; Aho, V. T. E.; Novikova, P. V.; Laczny, C. C.; Schneider, J. G. The Gut Microbiome Molecular Complex in Human Health and Disease. *Cell Host Microbe* **2022**, *30* (9), 1201−1206.
(4) Rowland, I.; Gibson, G.; Heinken, A.; Scott, K.; Swann, J.; Thiele, I.; Tuohy, K. Gut Microbiota Functions: Metabolism of Nutrients and Other Food Components. *Eur. J. Nutr.* **2018**, *57* (1), 1−24.
(5) Koropatkin, N. M.; Cameron, E. A.; Martens, E. C. How Glycan Metabolism Shapes the Human Gut Microbiota. *Nat. Rev. Microbiol.* **2012**, *10* (5), 323−335.
(6) Sugihara, K.; Kamada, N. Metabolic Network of the Gut Microbiota in Inflammatory Bowel Disease. *Inflamm. Regen.* **2024**, *44* (1), 11.
(7) Muramatsu, M. K.; Winter, S. E. Nutrient Acquisition Strategies by Gut Microbes. *Cell Host Microbe* **2024**, *32* (6), 863−874.
(8) Mills, R. H.; Dulai, P. S.; Vázquez-Baeza, Y.; Sauceda, C.; Daniel, N.; Gerner, R. R.; Batachari, L. E.; Malfavon, M.; Zhu, Q.; Weldon, K.; Humphrey, G.; Carrillo-Terrazas, M.; Goldasich, L. D.; Bryant, M.; Raffatellu, M.; Quinn, R. A.; Gewirtz, A. T.; Chassaing, B.; Chu, H.; Sandborn, W. J.; Dorrestein, P. C.; Knight, R.; Gonzalez, D. J. Multi-Omics Analyses of the Ulcerative Colitis Gut Microbiome Link Bacteroides Vulgatus Proteases with Disease Severity. *Nat. Microbiol.* **2022**, *7* (2), 262−276.
(9) McKee, L. S.; La Rosa, S. L.; Westereng, B.; Eijsink, V. G.; Pope, P. B.; Larsbrink, J. Polysaccharide Degradation by the Bacteroidetes: Mechanisms and Nomenclature. *Environ. Microbiol. Rep.* **2021**, *13* (5), 559−581.
(10) Flint, H. J.; Scott, K. P.; Duncan, S. H.; Louis, P.; Forano, E. Microbial Degradation of Complex Carbohydrates in the Gut. *Gut Microbes* **2012**, *3* (4), 289−306.
(11) Yüksel, E.; Voragen, A. G. J.; Kort, R. The Pectin Metabolizing Capacity of the Human Gut Microbiota. *Crit. Rev. Food Sci. Nutr.* **2025**, *65* (25), 1−23.
(12) Keung, W.-S.; Zhang, W.-H.; Luo, H.-Y.; Chan, K.-C.; Chan, Y.-M.; Xu, J. Correlation between the Structures of Natural Polysaccharides and Their Properties in Regulating Gut Microbiota: Current Understanding and Beyond. *Carbohydr. Polym.* **2025**, *352*, No. 123209.
(13) Bunesova, V.; Lacroix, C.; Schwab, C. Mucin Cross-Feeding of Infant Bifidobacteria and Eubacterium Hallii. *Microb. Ecol.* **2018**, *75* (1), 228−238.
(14) Arike, L.; Hansson, G. C. The Densely O-Glycosylated MUC2Mucin Protects the Intestine and Provides Food for the Commensal Bacteria. *J. Mol. Biol.* **2016**, *428* (16), 3221−3229.
(15) Berkhout, M. D.; Plugge, C. M.; Belzer, C. How Microbial Glycosyl Hydrolase Activity in the Gut Mucosa Initiates Microbial Cross-Feeding. *Glycobiology* **2022**, *32* (3), 182−200.
(16) Schroeder, B. O. Fight Them or Feed Them: How the Intestinal Mucus Layer Manages the Gut Microbiota. *Gastroenterol. Rep.* **2019**, *7* (1), 3−12.
(17) Tailford, L. E.; Crost, E. H.; Kavanaugh, D.; Juge, N. Mucin Glycan Foraging in the Human Gut Microbiome. *Front. Genet.* **2015**, *6*, 81.
(18) Glover, J. S.; Ticer, T. D.; Engevik, M. A. Characterizing the Mucin-Degrading Capacity of the Human Gut Microbiota. *Sci. Rep.* **2022**, *12* (1), 8456.
(19) Raba, G.; Luis, A. S. Mucin Utilization by Gut Microbiota: Recent Advances on Characterization of Key Enzymes. *Essays Biochem.* **2023**, *67* (3), 345−353.
(20) Johansson, M. E. V.; Gustafsson, J. K.; Holmén-Larsson, J.; Jabbar, K. S.; Xia, L.; Xu, H.; Ghishan, F. K.; Carvalho, F. A.; Gewirtz, A. T.; Sjövall, H.; Hansson, G. C. Bacteria Penetrate the Normally Impenetrable Inner Colon Mucus Layer in Both Murine Colitis Models and Patients with Ulcerative Colitis. *Gut* **2014**, *63* (2), 281−291.
(21) Kowalewski, M. E.; Redinbo, M. R. Emerging Gut Microbial Glycoside Hydrolase Inhibitors. *RSC Chem. Biol.* **2025**, 1233.
(22) Stubbs, K. A. Activity-Based Proteomics Probes for Carbohydrate-Processing Enzymes: Current Trends and Future Outlook. *Carbohydr. Res.* **2014**, *390*, 9−19.
(23) Wu, L.; Armstrong, Z.; Schröder, S. P.; de Boer, C.; Artola, M.; Aerts, J. M.; Overkleeft, H. S.; Davies, G. J. An Overview of Activity-Based Probes for Glycosidases. *Curr. Opin. Chem. Biol.* **2019**, *53*, 25−36.
(24) Killinger, B. J.; Whidbey, C.; Sadler, N. C.; DeLeon, A. J.; Munoz, N.; Kim, Y. M.; Wright, A. T. Activity-Based Protein Profiling Identifies Alternating Activation of Enzymes Involved in the Bifidobacterium Shunt Pathway or Mucin Degradation in the Gut Microbiome Response to Soluble Dietary Fiber. *Npj Biofilms Microbiomes* **2022**, *8* (1), 1−10.
(25) Chauvigné-Hines, L. M.; Anderson, L. N.; Weaver, H. M.; Brown, J. N.; Koech, P. K.; Nicora, C. D.; Hofstad, B. A.; Smith, R. D.; Wilkins, M. J.; Callister, S. J.; Wright, A. T. Suite of Activity-Based Probes for Cellulose-Degrading Enzymes. *J. Am. Chem. Soc.* **2012**, *134* (50), 20521−20532.
(26) Weerapana, E.; Simon, G. M.; Cravatt, B. F. Disparate Proteome Reactivity Profiles of Carbon Electrophiles. *Nat. Chem. Biol.* **2008**, *4* (7), 405−407.
(27) Ofman, T. P.; van der Marel, G. A.; Codée, J. D. C.; Overkleeft, H. S. Design and Synthesis of Exocyclic Cyclitol Aziridines as Potential Mechanism-Based Glycosidase Inactivators. *Eur. J. Org. Chem.* **2023**, *26* (16), No. e202300186.
(28) Artola, M.; Aerts, J. M. F. G.; van der Marel, G. A.; Rovira, C.; Codée, J. D. C.; Davies, G. J.; Overkleeft, H. S. From Mechanism-Based Retaining Glycosidase Inhibitors to Activity-Based Glycosidase Profiling. *J. Am. Chem. Soc.* **2024**, *146* (36), 24729−24741.
(29) de Boer, C.; McGregor, N. G. S.; Peterse, E.; Schröder, S. P.; Florea, B. I.; Jiang, J.; Reijngoud, J.; Ram, A. F. J.; van Wezel, G. P.; van der Marel, G. A.; Codée, J. D. C.; Overkleeft, H. S.; Davies, G. J. Glycosylated Cyclophellitol-Derived Activity-Based Probes and Inhibitors for Cellulases. *RSC Chem. Biol.* **2020**, *1* (3), 148−155.
(30) O'Brien, J. G. K.; Conway, L. P.; Ramaraj, P. K.; Jadhav, A. M.; Jin, J.; Dutra, J. K.; Evers, P.; Masoud, S. S.; Schupp, M.; Saridakis, I.; Chen, Y.; Maulide, N.; Pezacki, J. P.; am Ende, C. W.; Parker, C. G.; Fox, J. M. Mechanistic Differences between Linear vs. Spirocyclic

Dialkyldiazirine Probes for Photoaffinity Labeling. *Chem. Sci.* **2024**, *15* (37), 15463−15473.
(31) Homan, R. A.; Lapek, J. D.; Woo, C. M.; Niessen, S.; Jones, L. H.; Parker, C. G. Photoaffinity Labelling with Small Molecules. *Nat. Rev. Methods Primer* **2024**, *4* (1), 30.
(32) West, A. V.; Muncipinto, G.; Wu, H.-Y.; Huang, A. C.; Labenski, M. T.; Jones, L. H.; Woo, C. M. Labeling Preferences of Diazirines with Protein Biomolecules. *J. Am. Chem. Soc.* **2021**, *143* (17), 6691−6700.
(33) Bon, C.; Goretzki, B.; Flamme, M.; Shelton, C.; Davis, H.; Lima, F.; Garcia, F.; Brittain, S.; Brocklehurst, C. E. Oxadiazolines as Photoreleasable Labels for Drug Target Identification. *J. Am. Chem. Soc.* **2024**, *146* (39), 26759−26765.
(34) Herner, A.; Marjanovic, J.; Lewandowski, T. M.; Marin, V.; Patterson, M.; Miesbauer, L.; Ready, D.; Williams, J.; Vasudevan, A.; Lin, Q. 2-Aryl-5-Carboxytetrazole as a New Photoaffinity Label for Drug Target Identification. *J. Am. Chem. Soc.* **2016**, *138* (44), 14609−14615.
(35) Cheng, K.; Lee, J.-S.; Hao, P.; Yao, S. Q.; Ding, K.; Li, Z. Tetrazole-Based Probes for Integrated Phenotypic Screening, Affinity-Based Proteome Profiling, and Sensitive Detection of a Cancer Biomarker. *Angew. Chem., Int. Ed.* **2017**, *56* (47), 15044−15048.
(36) Zhao, S.; Dai, J.; Hu, M.; Liu, C.; Meng, R.; Liu, X.; Wang, C.; Luo, T. Photo-Induced Coupling Reactions of Tetrazoles with Carboxylic Acids in Aqueous Solution: Application in Protein Labelling. *Chem. Commun.* **2016**, *52* (25), 4702−4705.
(37) Thomas, R. P.; Grant, E. K.; Dickinson, E. R.; Zappacosta, F.; Edwards, L. J.; Hann, M. M.; House, D.; Tomkinson, N. C. O.; Bush, J. T. Reactive Fragments Targeting Carboxylate Residues Employing Direct to Biology, High-Throughput Chemistry. *RSC Med. Chem.* **2023**, *14* (4), 671−679.
(38) Martín-Gago, P.; Fansa, E. K.; Winzker, M.; Murarka, S.; Janning, P.; Schultz-Fademrecht, C.; Baumann, M.; Wittinghofer, A.; Waldmann, H. Covalent Protein Labeling at Glutamic Acids. *Cell Chem. Biol.* **2017**, *24* (5), 589−597.
(39) Bach, K.; Beerkens, B. L. H.; Zanon, P. R. A.; Hacker, S. M. Light-Activatable, 2,5-Disubstituted Tetrazoles for the Proteome-Wide Profiling of Aspartates and Glutamates in Living Bacteria. *ACS Cent. Sci.* **2020**, *6* (4), 546−554.
(40) Zanon, P. R. A.; Yu, F.; Musacchio, P. Z.; Lewald, L.; Zollo, M.; Krauskopf, K.; Mrdović, D.; Raunft, P.; Maher, T. E.; Cigler, M.; Chang, C. J.; Lang, K.; Toste, F. D.; Nesvizhskii, A. I.; Hacker, S. M. Profiling the Proteome-Wide Selectivity of Diverse Electrophiles. *Nat. Chem.* **2025**, *17* (11), 1712−1721.
(41) Luis, A. S.; Briggs, J.; Zhang, X.; Farnell, B.; Ndeh, D.; Labourel, A.; Baslé, A.; Cartmell, A.; Terrapon, N.; Stott, K.; Lowe, E. C.; McLean, R.; Shearer, K.; Schückel, J.; Venditto, I.; Ralet, M.-C.; Henrissat, B.; Martens, E. C.; Mosimann, S. C.; Abbott, D. W.; Gilbert, H. J. Dietary Pectic Glycans Are Degraded by Coordinated Enzyme Pathways in Human Colonic Bacteroides. *Nat. Microbiol.* **2018**, *3* (2), 210−219.
(42) Feng, J.; Qian, Y.; Zhou, Z.; Ertmer, S.; Vivas, E. I.; Lan, F.; Hamilton, J. J.; Rey, F. E.; Anantharaman, K.; Venturelli, O. S. Polysaccharide Utilization Loci in *Bacteroides* Determine Population Fitness and Community-Level Interactions. *Cell Host Microbe* **2022**, *30* (2), 200−215.
(43) Kleiner, P.; Heydenreuter, W.; Stahl, M.; Korotkov, V. S.; Sieber, S. A. A Whole Proteome Inventory of Background Photocrosslinker Binding. *Angew. Chem., Int. Ed.* **2017**, *56* (5), 1396−1401.
(44) Bakshani, C. R.; Ojuri, T. O.; Pilgaard, B.; Holck, J.; McInnes, R.; Kozak, R. P.; Zakhour, M.; Çakaj, S.; Kerouedan, M.; Newton, E.; Bolam, D. N.; Crouch, L. I. Carbohydrate-Active Enzymes from Akkermansia Muciniphila Break down Mucin O-Glycans to Completion. *Nat. Microbiol.* **2025**, *10* (2), 585−598.
(45) Prasch, H.; Wolfsgruber, A.; Thonhofer, M.; Culum, A.; Mandl, C.; Weber, P.; Zündel, M.; Nasseri, S. A.; Gonzalez Santana, A.; Tegl, G.; Nidetzky, B.; Gruber, K.; Stütz, A. E.; Withers, S. G.; Wrodnigg, T. M. Ligand-Directed Chemistry on Glycoside Hydrolases − A Proof of Concept Study. *ChemBioChem.* **2023**, *24* (23), No. e202300480.
(46) Cantarel, B. L.; Coutinho, P. M.; Rancurel, C.; Bernard, T.; Lombard, V.; Henrissat, B. The Carbohydrate-Active EnZymes Database (CAZy): An Expert Resource for Glycogenomics. *Nucleic Acids Res.* **2009**, *37* (Database), D233−D238.
(47) Lombard, V.; Golaconda Ramulu, H.; Drula, E.; Coutinho, P. M.; Henrissat, B. The Carbohydrate-Active Enzymes Database (CAZy) in 2013. *Nucleic Acids Res.* **2014**, *42* (D1), D490−D495.

https://doi.org/10.1021/acschembio.6c00268
ACS Chem. Biol. 2026, 21, 1496−1506